

## STRUCTURAL EVOLUTION OF METAMORPHIC AND INTRUSIVE ROCKS FROM THE CENTRAL PART OF THE SØR RONDANE MOUNTAINS, EAST ANTARCTICA

Tsuyoshi TOYOSHIMA<sup>1</sup>, Masaaki OWADA<sup>2</sup> and Kazuyuki SHIRAISHI<sup>3</sup>

<sup>1</sup>*Department of Geology, Faculty of Science, Niigata University,  
Ikarashi, Niigata 950-21*

<sup>2</sup>*Department of Mineral Science and Geology, Faculty of Science,  
Yamaguchi University, Yoshida, Yamaguchi 753*

<sup>3</sup>*National Institute of Polar Research, 9-10,  
Kaga 1-chome, Itabashi-ku, Tokyo 173*

**Abstract:** Structural evolution of the central part of the Sør Rondane Mountains (SRM) is divided into seven stages, from D<sub>1</sub> to D<sub>7</sub>, based on their characteristics of deformation, metamorphism and igneous activity. The metamorphic history of the central SRM is divided into three stages, prograde metamorphic peak stage, retrograde metamorphic stage related to its exhumation and contact metamorphic stage. The metamorphism of the former two stages has occurred not only with ductile deformation but also with various kinds of magmatic intrusions. The D<sub>1</sub> stage before the tonalite intrusion corresponds to the prograde metamorphic peak stage. The retrograde metamorphism and exhumation of the lower crustal rocks in the central SRM began at the D<sub>2</sub> stage, closely related to the tonalite intrusion and mylonitization. The D<sub>2</sub>-deformation and subsequent D<sub>3</sub>-mylonitization were caused by the top-to the SW to S and top-to the SE displacements, respectively, in extensional tectonic regimes.

After these mylonite-forming tectonics, poly-stage folding occurred in compressional tectonic regimes. The NNE-SSW compressional stress acted after the D<sub>3</sub> stage, resulting in the WNW-ESE trending folds and minor thrusts with top-to the N sense. The SRM rocks during this stage were emplaced under the greenschist-facies condition. Subsequently, the E-W compressional stress worked during the D<sub>5</sub> stage, and then NW-SE compression during the D<sub>6</sub> stage. Granites and syenites intruded in the last stage. Strain-free quartz ribbon and random-oriented kyanites and biotites might have been produced by the contact metamorphism with the non-foliated 500 Ma granites.

### 1. Introduction

High- and medium-grade metamorphic rocks and many kinds of igneous rocks crop out in the Sør Rondane Mountains (SRM), Queen Maud Land (22° to 28°E longitude), East Antarctica. Belgian and Japanese geologists have carried out field surveys and outlined the geology of the mountains (VAN AUTENBOER, 1969; VAN AUTENBOER and LOY, 1972; KOJIMA and SHIRAISHI, 1986; ISHIZUKA and KOJIMA, 1987; SHIRAISHI *et al.*, 1991, 1992). Moreover, petrological and petrochemical studies have been performed by many authors (*e.g.* ASAMI and SHIRAISHI, 1987; SAKIYAMA *et al.*, 1988; OSANAI *et al.*, 1991, 1992).

However, the structural geology of the mountains is not so clear and only few authors have discussed the tectonic processes of formation of the SRM rocks (*e.g.* OSANAI *et al.*, 1991, 1992; TOYOSHIMA *et al.*, 1991). The present authors have performed a detailed geological survey in the central part of the SRM (25°E longitude), as members of the Japanese Antarctic Research Expedition (JARE-32, -31). This paper describes the structures of the SRM rocks and reveals their deformation history and related intrusive history. Movement picture of the SRM rocks will also be synthesized on individual deformation stages. Mineral abbreviations used are after KRETZ (1983).

## 2. Outline of Geology

The central part of the SRM is underlain largely by Neoproterozoic granulite and amphibolite to greenschists-facies metamorphic rocks and Neoproterozoic to early Cambrian plutonic rocks containing minor dikes (*e.g.* KOJIMA and SHIRAIISHI, 1986; ISHIZUKA and KOJIMA, 1987; SHIRAIISHI *et al.*, 1991, 1992; OSANAI *et al.*, 1992). The metamorphic rocks can be divided into two terranes on the basis of the metamorphic peak conditions: northeastern (NE) and southwestern (SW) terranes (OSANAI *et al.*, 1992). The former is rich in psammitic to pelitic gneisses associated with amphibolites and calc-silicate gneisses (ASAMI *et al.*, 1992; SHIRAIISHI *et al.*, 1991, 1992; OSANAI *et al.*, 1992; ISHIZUKA *et al.*, 1993). They have orthopyroxene or related granulite facies mineral assemblages such as Sil + Grt + Bt ± Crd + Pl + Kfs + Qtz and Opx + Cpx + Grt + Hbl + Pl + Qtz (ASAMI *et al.*, 1992; SHIRAIISHI *et al.*, 1991, 1992; OSANAI *et al.*, 1992; ISHIZUKA *et al.*, 1993). The latter terrane consists mainly of metatonalites and basic gneisses which have amphibolite facies mineral assemblages such as Hbl + Bt ± Grt + Pl ± Qtz (SHIRAIISHI *et al.*, 1991, 1992).

By using various geothermo-barometers, the metamorphic *P-T* conditions have been estimated to be 750° to 850°C and 700 to 800 MPa for non-mylonitized gneisses, and 530° to 630°C and 500 to 550 MPa for mylonitized gneisses in the granulite facies NE terrane (SHIRAIISHI and KOJIMA, 1987; ASAMI and SHIRAIISHI, 1987; OSANAI *et al.*, 1988, 1992; ASAMI *et al.*, 1992). ASAMI *et al.* (1992) divided metamorphic evolution of the SRM into four metamorphic stages on the basis of detailed petrological study: prograde, main (metamorphic peak), retrograde and contact metamorphic stages. The metamorphic grade after the main stage decreases from granulite facies to greenschist facies after contact metamorphism with non-foliated granitic intrusives.

Foliation of metamorphic rocks generally trends E-W to NE-SW and dips southward in the western part of the SRM (SHIRAIISHI *et al.*, 1992). But it trends variously in the central part of the SRM (Figs. 1 and 2) as well as the eastern part where NE-SW and NW-SE trending folds develop (ISHIZUKA *et al.*, 1993). The central part of the SRM is characterized by a few stages of fold (Figs. 1 and 2). Discontinuity of fold axes of WNW-ESE trending antiform and synform implies a N-S trending fault in the central SRM (shown by a broken line in Fig. 1), as shown by SHIRAIISHI *et al.* (Fig. 1, 1991).

## 3. Deformation History of the Central Sør Rondane Mountains

Tectonism and metamorphism of a metamorphic belt is generally understood in terms of the *P-T-t-D* path of the constituent units. The first step of the *P-T-t-D* path analysis is

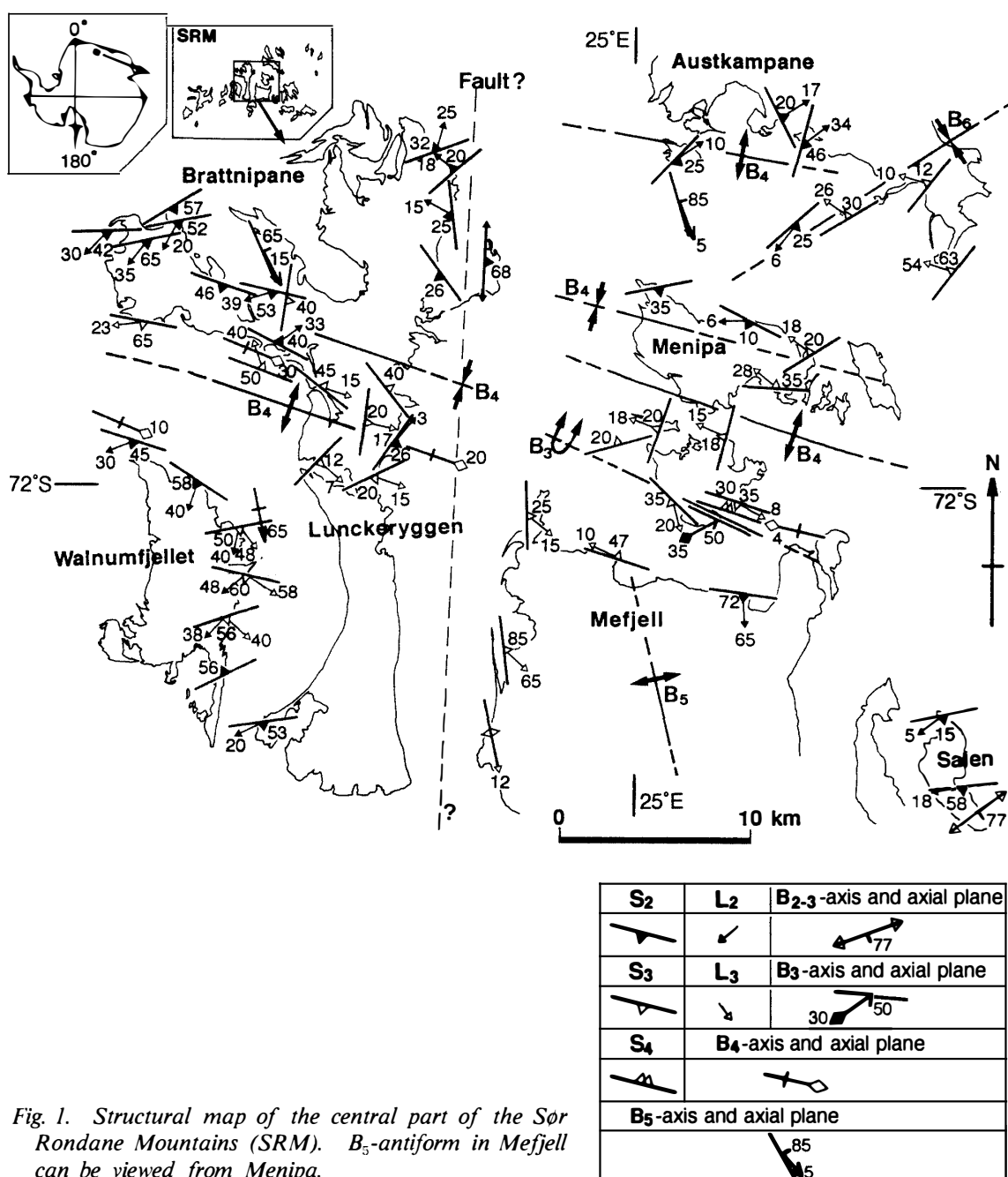
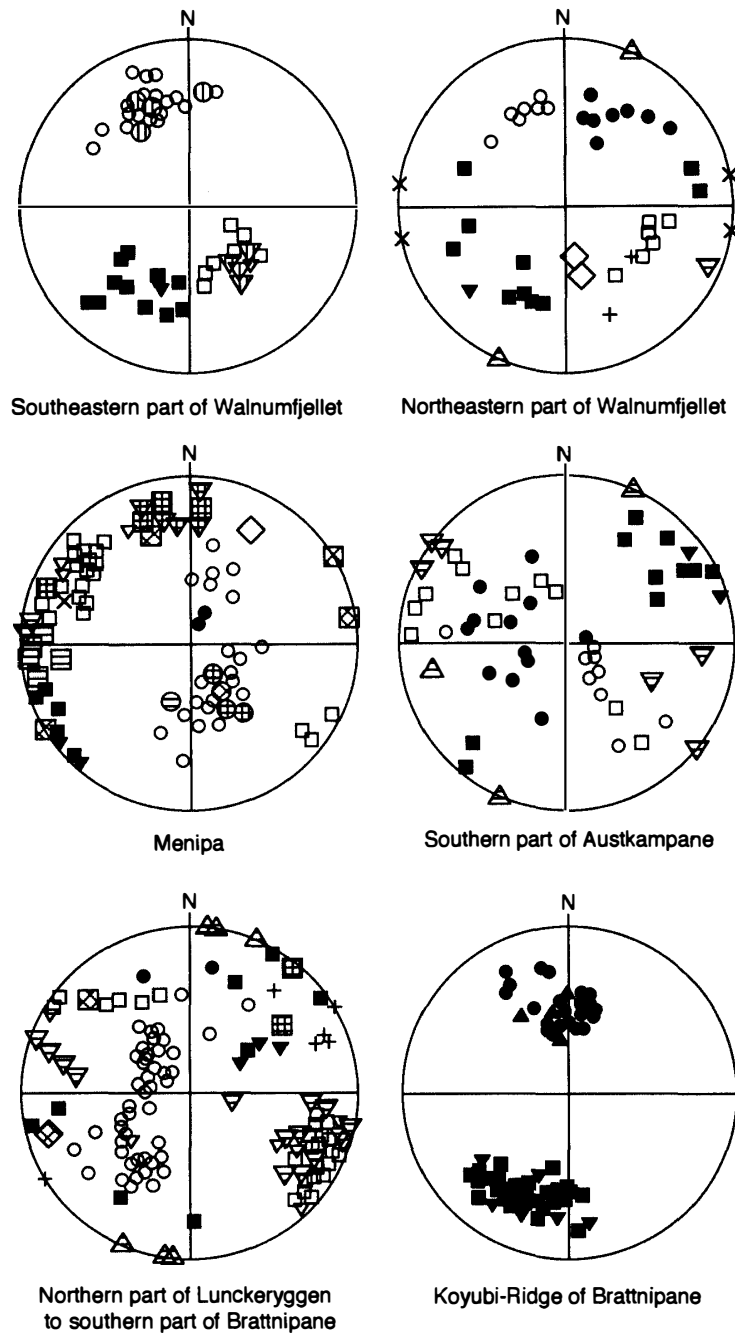


Fig. 1. Structural map of the central part of the Sør Rondane Mountains (SRM). B<sub>5</sub>-antiform in Meffjell can be viewed from Menipa.

to clarify the deformation history.

Rock structures and mineral textures in the central SRM rocks were formed through multiphase deformation, as outlined in Table 1. Seven stages of deformation are recognized, alternating between ductile (folding and formation of foliation) and brittle deformations (fracturing and faulting). The deformations of three early stages (D<sub>2</sub> to D<sub>4</sub>) are of penetrative type (Fig. 1), but those of three later stages (D<sub>5</sub> to D<sub>7</sub>) are not of penetrative type. Rock-fracturing and faulting were associated with magmatic intrusions and minor shear zones. Because each stage of deformation is associated with metamorphism and in



Stage	D <sub>1</sub>	D <sub>1-3</sub>	D <sub>2</sub>	D <sub>3</sub>	D <sub>4</sub>	D <sub>5</sub>	D <sub>6</sub>
Pole of foliation	⊗	⊕	●	○	⊖	◇	
Mineral lineation	⊗	⊕	■	□	⊖		
Fold axis		▽	▽	▽	▽	◇	+
Pole of axial plane of fold			▲		▲	×	
Pole of shear plane of minor shear zone					⊖		
Mineral lineation in shear zone					▽		

Fig. 2. Lower hemisphere equal area projections of foliations (S), mineral lineations (L) and fold axes (B) within the central Sør Rondane Mountains.

Table 1. Deformation history of the central part of the Sør Rondane Mountains.

Deformation event	Structure	Magmatism	Metamorphism	Movement picture	Age (Ma)
D <sub>1</sub>	banding-parallel foliation (S <sub>1</sub> ) with boudins, tight to isoclinal fold (B <sub>1</sub> )		peak of prograde metamorphism ? granulite to amphibolite facies ?		1000*
D <sub>2</sub>	fracture filled with tonalite and gabbro intrusives, mylonitic foliation (S <sub>2</sub> ) and tight fold (B <sub>2</sub> )	tonalitic and gabbroic	amphibolite facies	top-to the SW to S displacement formation of the MSZ	950**
D <sub>3</sub>	mylonitic foliation (S <sub>3</sub> ), minor tight fold (B <sub>3</sub> ) and major recumbent fold (B <sub>3</sub> )	pegmatite I and granitic	retrograde metamorphism	top-to the SE displacement formation of the SRS	
D <sub>4</sub>	WNW-ESE trending open to tight fold (B <sub>4</sub> ), minor shear zone and fracture filled with intruded granitic rock	pegmatite II	greenschist facies	N-S trending compression and northward thrusting ?	
D <sub>5</sub>	N-S trending open to gentle fold (B <sub>5</sub> )			E-W trending compression	
D <sub>6</sub>	NE-SW trending gentle fold (B <sub>6</sub> )			NW-SE trending compression	
D <sub>7</sub>	fracture filled with intruded syenitic and granitic rocks	syenitic and granitic			500**

\*SHIRAIISHI and KAGAMI (1989), \*\*TAKAHASHI *et al.* (1990).

MSZ: Main Shear Zone (KOJIMA and SHIRAIISHI, 1986).

SRS: Sør Rondane Suture (OSANAI *et al.*, 1992).

some cases with magmatic intrusion, the deformation history is intimately related to the metamorphic and magmatic history.

### 3.1. Deformation before tonalite intrusion (D<sub>1</sub>-stage)

The deformation stage (D<sub>1</sub> stage) before tonalite intrusion is characterized by the formation of lithological banding-parallel foliation (S<sub>1</sub>) with boudins and by tight to isoclinal folding of the S<sub>1</sub>-foliation but not by mylonitization. Most of the D<sub>1</sub>-structures appear to have strongly lost their initial structural characteristics owing to overprinting of subsequent deformation such as mylonitization and folding. The subsequent deformations were associated with retrograde recrystallization of metamorphic minerals and with contact metamorphism by the latest non-foliated granite intrusion. Therefore, the trace of the D<sub>1</sub>-stage metamorphism was also frequently lost during the later events associated with mylonitization.

The metamorphic peak *P-T* conditions of pelitic gneisses have been estimated to be about 750° to 850°C and 700 to 800 MPa in the NE terrane (ASAMI and SHIRAIISHI, 1987;

OSANAI *et al.*, 1988). The present authors regard the  $P$ - $T$  sets as the conditions of the  $D_1$ -stage, because the gneisses are not mylonitized. Thus, the  $D_1$ -deformation may be synchronous with the peak of prograde metamorphism of the SRM rocks. Granulite facies basic gneisses yielded Rb-Sr and Sm-Nd whole rock isochron ages of ca. 1000 Ma, which has been regarded as the age of the granulite-facies regional metamorphic peak in the SRM (SHIRAISHI and KAGAMI, 1989).

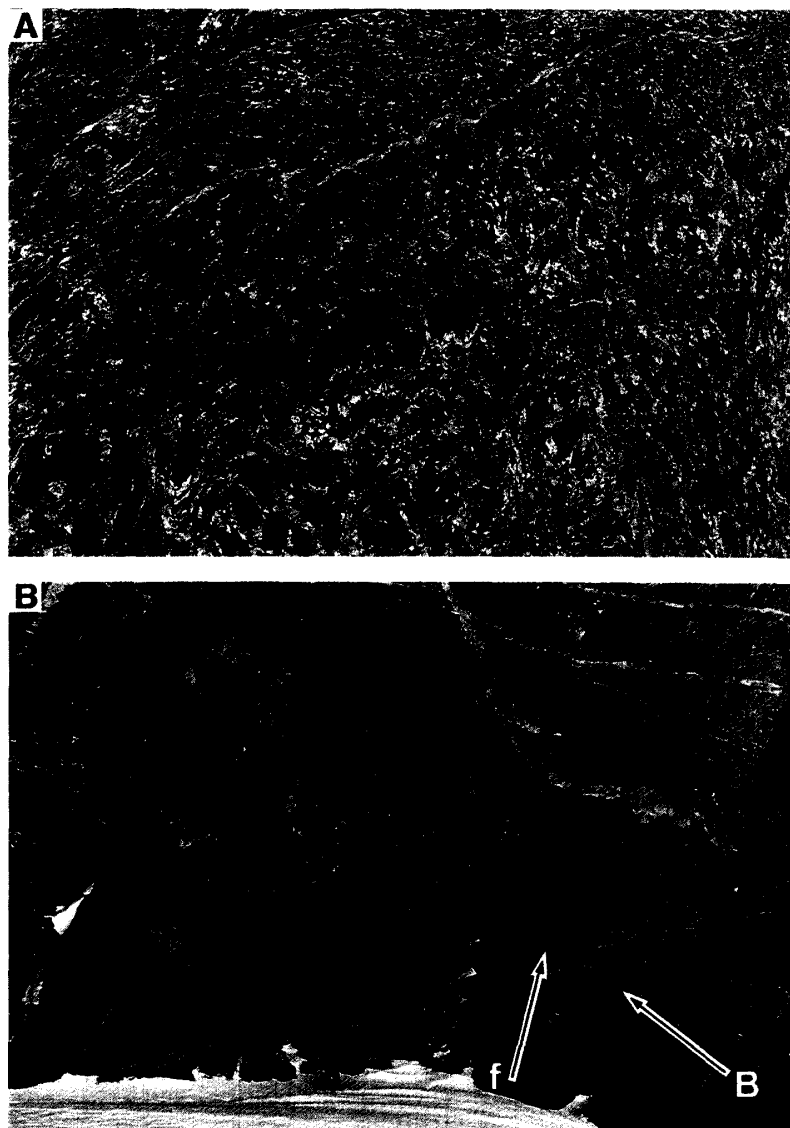


Fig. 3. A.  $B_1$ -boudins (dark colored) (B) in biotite gneiss (light colored) rotated (r), folded (f) and shortened (s) by  $D_2$ -folding in the southern part of Salen (locality no. 91012204). Dark colored boudins and lenses vary in length from 5 to 20 cm. B.  $B_2$ -fold of  $S_1$ -foliation with  $S_1$ -boudins (B), cut by  $D_3$ -pegmatite (Pm, pegmatite I after OWADA *et al.*, 1991, 1992) in the southern part of Salen (locality no. 91012203). After the pegmatitic intrusion, the interlimb angles of the  $B_2$ -fold progressively decreased owing to the  $B_3$ -folding. The  $S_1$ -boudins are folded (f) and rotated by the  $D_2$ - and  $D_3$ -foldings.

### 3.1.1. Boudinage ( $S_1$ -phase)

The earliest phase ( $S_1$ -phase) of deformation in the SRM rocks is defined by  $S_1$ -foliation with boudins. The  $S_1$ -boudins are quartzo-feldspathic veins and thin layers of coarse-grained amphibolite intercalated within fine-grained amphibolites, pelitic-psammitic and charnockitic gneisses. Most of the  $S_1$ -boudin and -foliation are folded and rotated by deformation after tonalite intrusion (Fig. 3).

### 3.1.2. Tight to isoclinal folding ( $S_1'$ -phase)

The deformation of the  $S_1'$ -phase is characterized by the folding of the  $S_1$ -foliation in tight to isoclinal shapes ( $B_1'$ ) with well developed axial foliation ( $S_1'$ ). The  $B_1'$ -folds are cut across by tonalite dykes (Fig. 4A). The tonalites rarely contain metamorphic inclu-

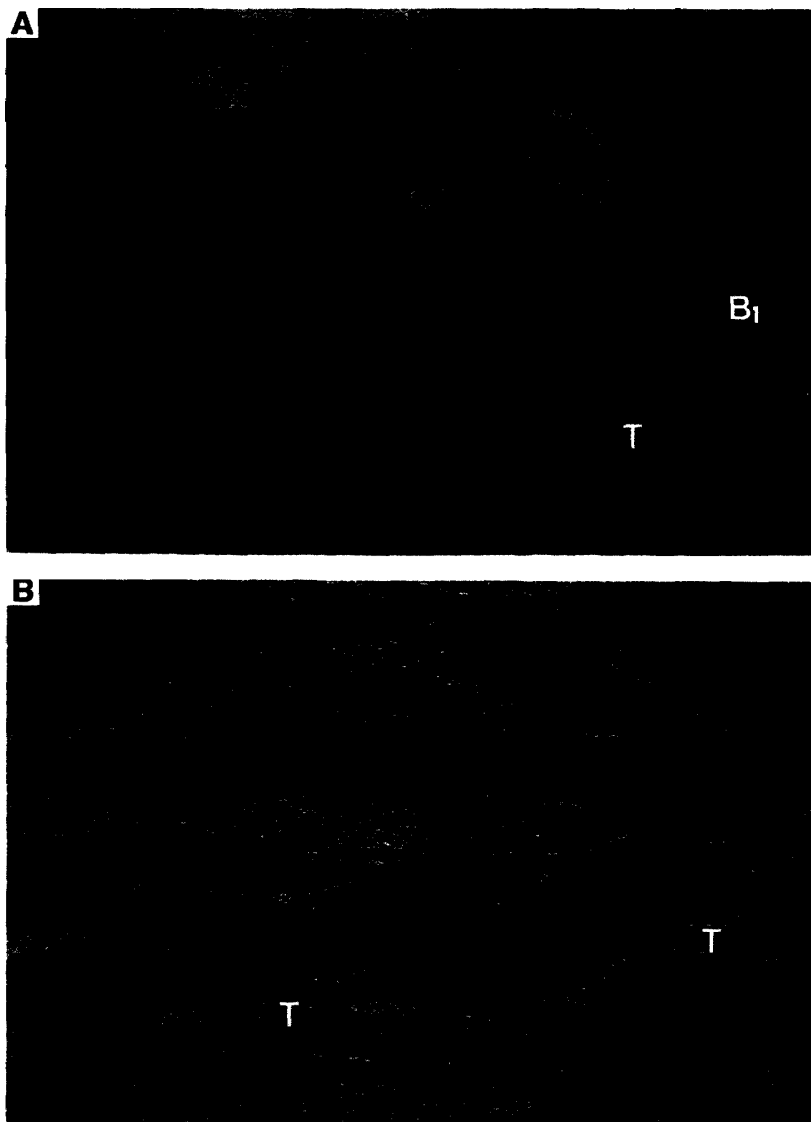


Fig. 4.  $D_2$ -tonalite. A.  $B_1$ -isoclinal fold ( $B_1$ ) in calc-silicate gneiss intruded and cut by  $D_2$ -tonalite (T) in the southernmost part of Lunckeryggen (locality no. 90010208). B.  $D_2$ -tonalite veins (T) injected along shear fractures into biotite-hornblende gneiss (dark colored) in the northwestern part (Kusuriyubi Ridge) of Brattnipane (locality no. 90122801).

sions that preserve  $B_1'$ -folds.

### 3.2. *Top-to the SW to S displacement associated with retrograde mylonitization and tonalite intrusion ( $D_2$ stage)*

The deformation of the  $D_2$  stage is characterized by tonalite intrusion, the formation of  $S_1$ -parallel mylonitic foliation ( $S_2$ ) and folding of the  $S_1$ - and  $S_1'$ -foliations ( $B_2$ ) with well developed axial foliation ( $S_2$ ). The  $D_2$ -tonalitic intrusives cut  $S_1$ - and  $S_1'$ -foliations (Fig. 4). The  $S_2$ -foliations trend E-W to ENE-WSW and dip southward with NE-SW to N-S trending mineral lineation ( $L_2$ ) (Figs. 1 and 2). The  $L_2$ -lineation is frequently cut across by NW-SE trending mineral lineation ( $L_3$ ) on another mylonitic foliation ( $S_3$ ) formed after the  $D_2$  stage. Moreover, some of the  $L_3$ -lineations curve from a NE-SW trend toward a NW-SE trend showing a U-shape. The  $D_2$ -structures are cut by leucocratic granite and pegmatite (Fig. 3B) (pegmatite I after OWADA *et al.*, 1991, 1992) which were folded and/or mylonitized during the  $D_3$  stage. The  $D_2$ -structures are folded by post- $D_2$  folding (Figs. 1 and 2), with tight to isoclinal shape and NW-SE trending fold axis (Fig.

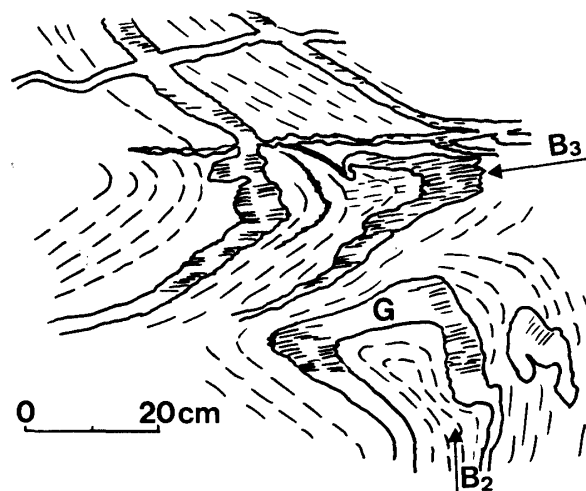


Fig. 5.  $B_2$ -fold ( $B_2$ ), shown by granitic vein ( $G$ ), refolded by  $B_3$ -fold ( $B_3$ ) at the southern end of Brattnipane (locality no. 91010602).

5) and with open to tight shape and WNW-ESE trending fold axis (Fig. 14).

Most of the  $D_2$ -intrusives show tonalitic affinity, though partly gabbroic and granitic (OWADA *et al.*, 1991, 1992; SHIRAISHI *et al.*, 1991, 1992). The tonalites are mainly made up of hornblende, biotite, plagioclase and quartz. The gabbros are composed mainly of hornblende and plagioclase, and the granites are mainly made up of biotite, plagioclase, quartz and alkali feldspar. Almost all of the  $D_2$ -intrusive rocks have  $S_2$ -mylonitic foliation and  $L_2$ -mineral lineation, showing that they, together with surrounding metamorphic rocks and contained metamorphic inclusions, were deformed immediately after the intrusion. Structures of the  $D_2$  stage are prominent structures in the central SRM. Only a little  $D_2$ -intrusive rock in the southern part of the SRM does not show mylonitic foliation and lineation, and contains metamorphic rock blocks which have  $S_1'$ -foliation (Fig. 4A). The  $D_2$ -intrusives of the SRM are cut by pegmatites, syenites and granites (OWADA *et al.*, 1991, 1992; SAKIYAMA *et al.*, 1988).

The main masses of  $D_2$ -tonalites occur as parallel large-scale sheets in an E-W trending zone (SHIRAISHI *et al.*, 1991, 1992). The northern edge of the zone was named the Main Shear Zone because the tonalites are strongly mylonitized after their intrusion (KOJIMA and SHIRAISHI, 1986). The tonalite sheets are parallel to the  $S_2$ -mylonitic foliation. Many  $D_2$ -tonalite veins are injected along shear fractures (Fig. 4B). These imply that the tonalite intruded into a regional fracture zone at first, and then the zone functioned as a mylonite zone. The tonalite intrusion may have occurred in the same series of movements as the mylonitization. The  $D_2$ -mylonites show various kinds of asymmetrical structures such as rotated boudins of amphibolites (Fig. 6), S-C structures (BERTHÉ *et al.*, 1979; LISTER and SNOKE, 1984) and  $C'$  surfaces (PONCE DE LEON and CHOUKROUNE, 1980) (Figs. 7A and B)

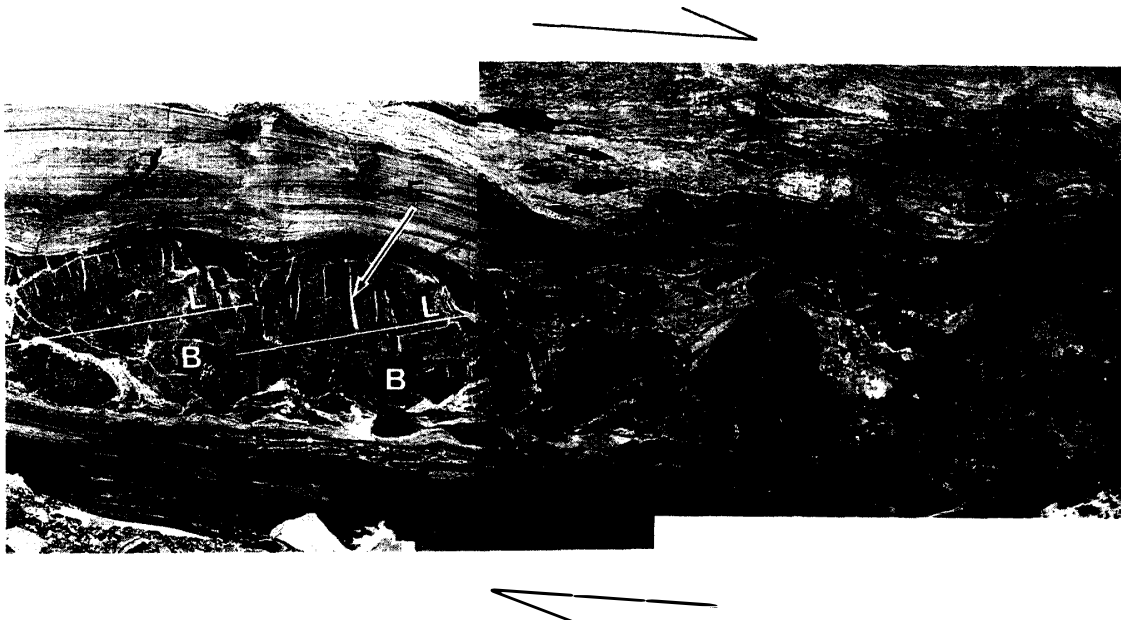


Fig. 6. Sinistrally rotated boudins (B) of amphibolite in mylonites derived from Bt-Hbl gneiss and  $D_3$ -granitic rock in the northern part of Lunckeryggen (locality no. 91010501). Long axis (L) of individual boudin is oblique to the enclosing mylonite with a low angle. Extension fracture (E) is filled with quartz vein. Top-to-the-SW sense of shear.

as well as porphyroclasts with asymmetrical tails of recrystallized fine-grained minerals (Fig. 7C). These structures indicate that the deformation of the  $D_2$  stage was caused by a top-to-the SW to S sense of shear.

The  $D_2$ -mylonitization also developed folding of  $D_2$ -tonalite dykes and veins in tight to open shapes with  $S_2$ -axial foliation. The  $B_2$ -folds of pre- $S_2$ -foliations show tight to isoclinal shapes. Some folds are of asymmetric type and show rootless forms, owing to a high-strain magnitude during the folding. In some places the  $D_2$ -folding progressively induced decrease of interlimb angles of  $B_1'$ -folds (Fig. 8).

The  $S_2$ -mylonitic foliation and  $L_2$ -mineral lineation in the  $D_2$ -tonalites are mainly defined by Hbl+Bt+Pl+Qtz (Fig. 7B), in pelitic to psammitic mylonites by Bt±Sil+Qtz+Pl±Kfs (Fig. 7C) and in intermediate to basic mylonites by Hbl±Bt+Pl±Qtz. In the SW terrane, the  $D_2$ -structures are defined by the same mineral assemblages as pre- $D_2$ -structures. Orthopyroxene and related granulite facies mineral assemblages are not found

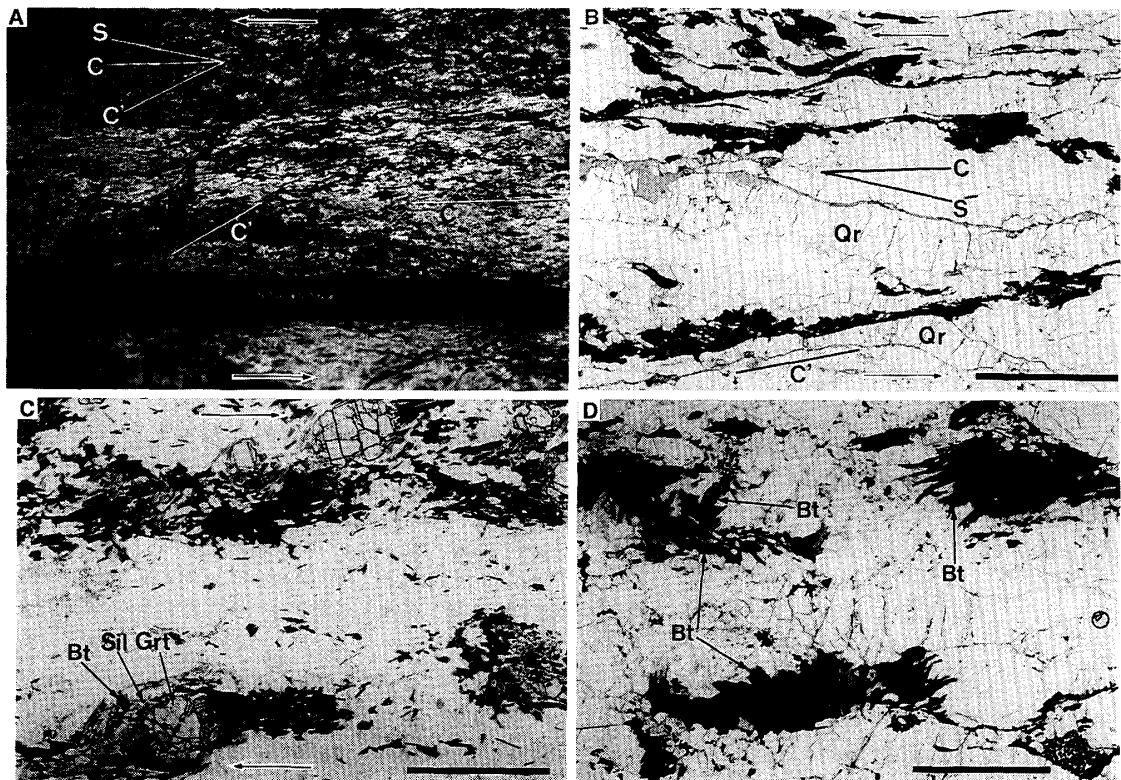


Fig. 7. Deformation structures and textures of  $D_2$ -deformed rocks. Top-to-the-SW sense of shear. A and B. S-C-C' mylonites derived from  $D_2$ -tonalite and Bt-Hbl gneiss. A is found in the southeastern part of Walnumfjellet (locality no. 90123004). B. Quartz ribbons (Qr) are strongly elongated oblique to  $S_2$ -foliation but consist of subequant to equigranular quartz grains in the Bt-Hbl mylonite from the northwestern part (Koyubi Ridge) of Brattnipane (sample no. 90122603-B-TB-6). The scale bar is 2.0 mm. Plane-polarized light (PPL). C. Garnet porphyroclast (Grt) with asymmetrical tails of recrystallized fine-grained sillimanite (Sil), biotite (Bt) and quartz in pelitic mylonite from the southern end of Austkampane (sample no. T91020102C). The scale bar is 2.0 mm. PPL. D. Random-oriented biotite grains (Bt) cutting mylonitic foliation in  $D_2$ -mylonite from the northwestern part (Koyubi Ridge) of Brattnipane (sample no. 90122603-D-TB-6). The scale bar is 1.0 mm. PPL.

in the foliated  $D_2$ -tonalite and host metamorphic rocks of the NE terrane which were suffered by  $D_2$ -mylonitization and post- $D_2$  stage deformations. The sillimanite and biotite defining  $S_2$  resulted from the breakdown of garnet porphyroclast in pelitic mylonite from the NE terrane (Fig. 7C). These show that during the  $D_2$  stage, retrograde amphibolite facies mylonitization occurred in the granulite facies NE terrane. On the other hand, the amphibolite facies SW terrane during the  $D_2$  stage appears to have mylonitized under the same amphibolite facies conditions as its metamorphic peak. SHIRAIISHI *et al.* (1991) pointed out in the petrological study that in the SW terrane, the tonalites were emplaced immediately after the peak regional metamorphism and that they were metamorphosed and mylonitized during the retrograde stage. This suggests that the  $D_2$ -magmatic intrusion and -mylonitization caused the metamorphic rocks of the SRM to be detached and exhumed from the lower crust immediately after the granulite and amphibolite facies metamorphic peaks.

Tonalites of the  $D_2$  stage yielded a Rb-Sr whole rock isochron age of 950 Ma, which has been regarded as the age of the tonalite intrusion (TAKAHASHI *et al.*, 1990). This age is conformable with the above interpretation that the  $D_2$ -tonalite intrusion occurred after the 1000 Ma granulite facies metamorphism in the NE terrane of the SRM.

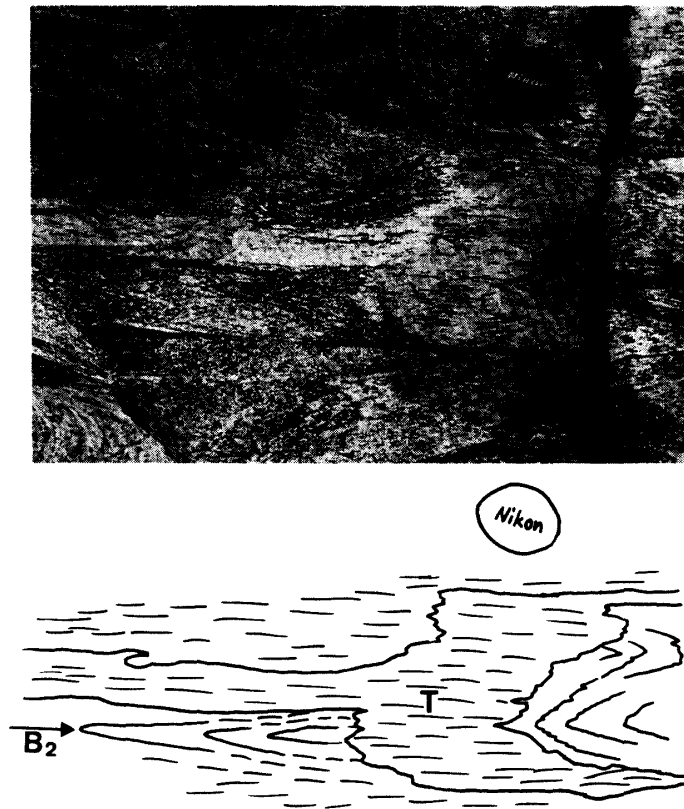


Fig. 8.  $B_{2-3}$ -fold ( $B_2$ ) developed from  $D_1$  to  $D_2$  stages at the northeastern corner of Walnumfjellet (locality no. 91010301).  $D_2$ -tonalite (T), intruding  $D_1$ -folded gneiss, was deformed by  $B_2$ -folding. Lens cap of camera is 5.2 cm in diameter.

### 3.3. *Top-to the SE displacement associated with retrograde mylonitization and minor magmatic intrusion (D<sub>3</sub> stage)*

The deformation of the D<sub>3</sub> stage is characterized by the amphibolite facies mylonitization developed S<sub>2</sub>-parallel mylonitic foliation (S<sub>3</sub>) with NW-SE trending mineral lineation (L<sub>3</sub>), by refolding (B<sub>3</sub>) of B<sub>2</sub>-folds (Fig. 5) and by dioritic to granodioritic intrusion. Structures of the D<sub>3</sub> stage are prominent ones in the central SRM. The L<sub>3</sub>-lineation on the S<sub>3</sub>-foliation cuts L<sub>2</sub>-lineation. The D<sub>3</sub>-structures are folded with open to tight shape and WNW-ESE trending fold axis by post-D<sub>3</sub> folding (Figs. 1, 2, 9 and 10).

D<sub>3</sub>-mylonites show various kinds of asymmetrical structures such as S-C structures and C' surfaces as well as porphyroclasts with asymmetrical tails of recrystallized fine-grained minerals (Figs. 11A and B). These structures indicate that the deformation of the D<sub>3</sub> stage was caused by a top-to the SE sense of shear.

The D<sub>3</sub>-mylonitization also developed folding of pre-D<sub>3</sub>-structures in tight to isoclinal shapes with well developed axial foliation (S<sub>3</sub>) (Fig. 5). Some B<sub>3</sub>-folds are of large-scale recumbent type with isoclinal shape and NE-SW trending fold axis (Figs. 1 and 12). The S<sub>3</sub>-axial foliation is generally parallel or sub-parallel to the S<sub>3</sub>-mylonitic foliation. Most axes of the B<sub>3</sub>-fold are parallel to L<sub>3</sub>-lineation. In some places the D<sub>3</sub>-folding progressively resulted in decrease of the interlimb angles of B<sub>2</sub>-folds (Fig. 3B).

The D<sub>3</sub>-structures are defined by the same mineral assemblages as the D<sub>2</sub>-structures. This suggests that the D<sub>3</sub>-deformation occurred under the same amphibolite facies metamorphic conditions as the D<sub>2</sub>-deformation. The D<sub>3</sub> stage after the present authors corresponds in movement and metamorphic conditions to the mylonite-forming event after OSANAI *et al.* (1988). Therefore, the Sør Rondane Suture (OSANAI *et al.*, 1991) was formed during the D<sub>3</sub> stage. ASAMI and SHIRAISHI (1987), OSANAI *et al.* (1988) and ASAMI *et al.* (1992) suggest that the metamorphic conditions of the D<sub>2</sub> to D<sub>3</sub> stages were 530° to 580°C and 550 to 450 MPa in the central part of the SRM.

### 3.4. *NNE-SSW compression resulting in WNW-ESE trending fold (D<sub>4</sub> stage)*

The deformation of the D<sub>4</sub> stage is characterized by the formations of WNW-ESE trending fold (B<sub>4</sub>) of the pre-D<sub>4</sub>-foliations and of fractures filled with pegmatitic intrusives (Figs. 1 and 2). The B<sub>4</sub>-folds form open to tight shapes with subvertical axial foliation (S<sub>4</sub>) (Figs. 13 and 14). The pegmatitic dykes and veins are often intruded along the axial foliation (pegmatite II after OWADA *et al.*, 1991, 1992) (Fig. 13). Some of the folds show geological map scale antiform and synform (Fig. 1). The B<sub>4</sub>-fold refolds the pre-B<sub>4</sub>-fold (Figs. 13 and 14). These D<sub>4</sub>-structures are deformed by folding in open to gentle shapes with axial foliation (S<sub>5</sub>) (Fig. 16). The D<sub>4</sub>-folding may have resulted from NNE-SSW compression. Chl + Ms + Qtz and Chl + Epi ± Qtz define the S<sub>4</sub>-axial foliation, suggesting D<sub>4</sub>-deformation under greenschist facies metamorphic conditions.

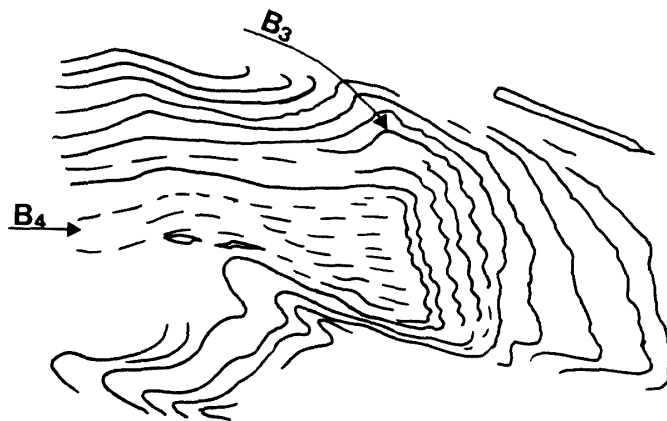
Minor shear zones trending WNW-ESE and dipping steeply southward are developed where the S<sub>3</sub>-foliation is steeply inclined to the south, especially in the SW terrane. The minor shear zones cut across and deflect the S<sub>3</sub>-foliation (Fig. 15). The shear zone with the deflection of S<sub>3</sub>-foliation has a monoclinic symmetry and a top-to-the-N shear sense along steeply southward-inclined planes in a NNE-SSW compressional tectonic regime (Fig. 15). The shear zones are defined by the same greenschist facies mineral assemblages as the S<sub>4</sub>-axial foliation. Therefore the WNW-ESE trending fold and minor shear zones



Fig. 9.  $B_3$ -fold ( $B_3$ ), defined by the mafic layer, refolded by  $B_4$ -fold ( $B_4$ ) at the southern end of Menipa (locality no. 91012504).



Fig. 10.  $B_3$ -fold ( $B_3$ ) refolded by  $B_4$ -fold at the southern end of Menipa (locality no. 91012504). Axis of the  $B_3$ -fold are curved toward the orientation parallel to the  $B_4$ -fold axis.



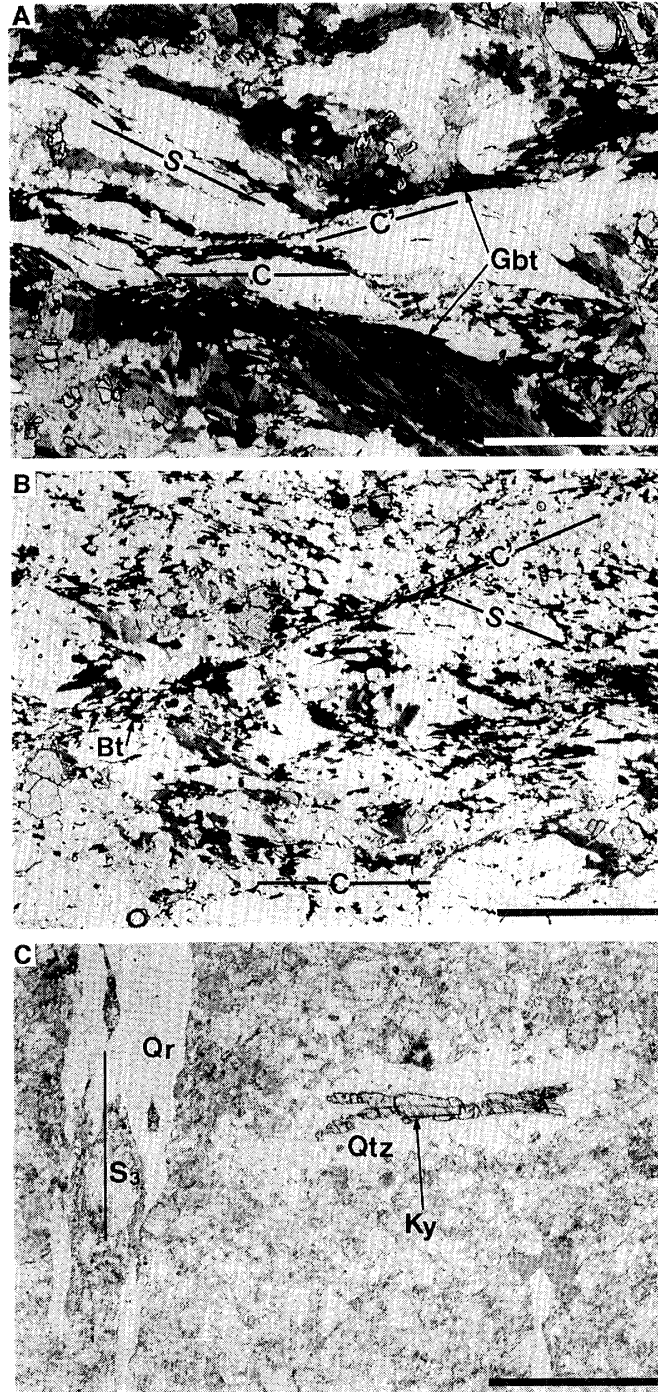


Fig. 11. Microphotographs of  $D_3$ -deformed rocks. The scale bar is 2.0 mm. Plane-polarized light. A. Pelitic mylonite with S-C-C' fabrics defined by green biotite (Gbt) from the southern end of Brattnipane (sample no. T91010603A). Top-to-the-SE sense of shear. B. Weakly preferred orientation of fine-grained biotite (Bt) in  $D_3$ -pelitic mylonite from the central part of Menipa (sample no. T910124-T09-B). Asymmetrical microstructure such as S-C-C' fabrics in the mylonite is unclear. C. Kyanite (Ky) + quartz (Qtz) porphyroblast cutting  $S_3$ -mylonitic foliation ( $S_3$ ) at the southern end of Brattnipane (sample no. T90123101). The foliation is defined by quartz ribbon (Qr).

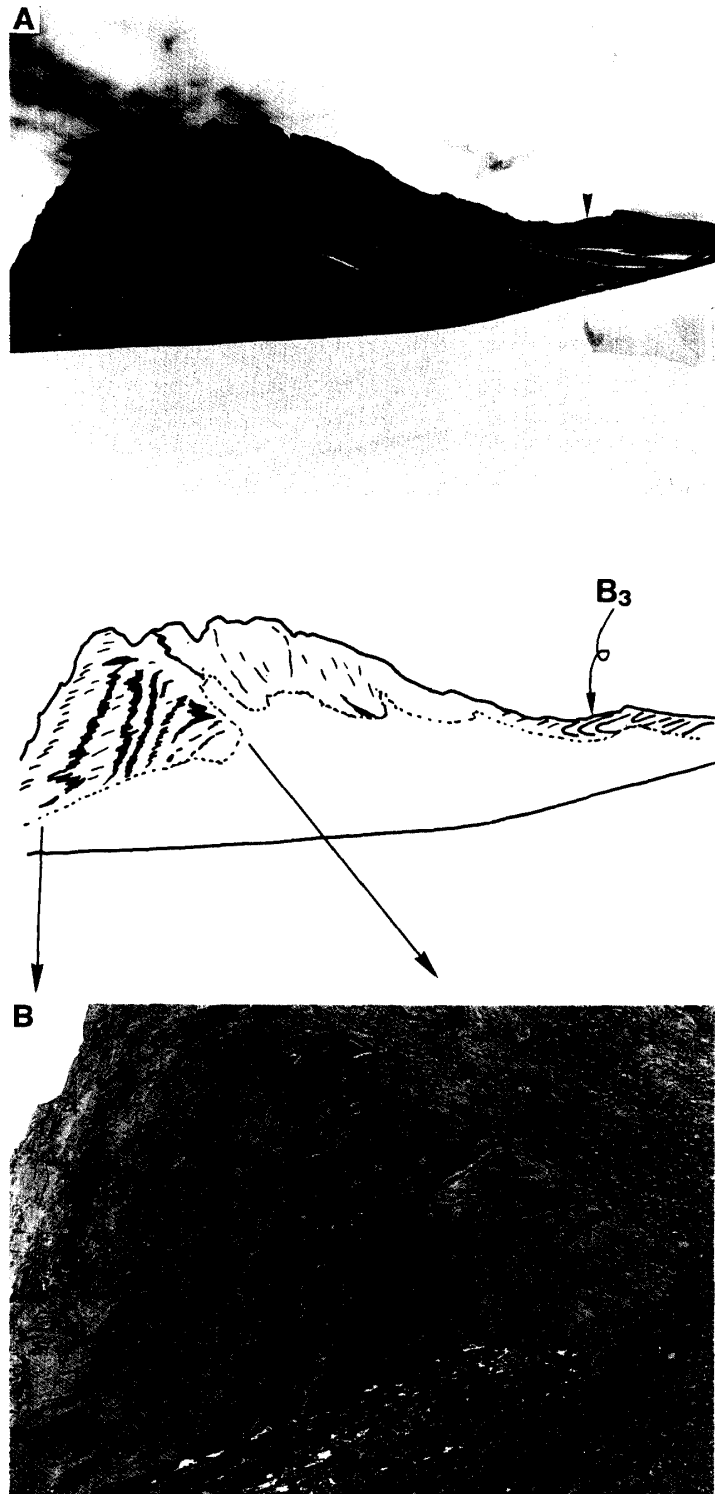


Fig. 12. A. Photograph and sketch of  $B_3$ -large-scale recumbent fold ( $B_3$ ) with isoclinal shape, defined by mafic layer in the southern part of Menipa (locality no. 91012504). The cliff height is about 320 m. B. Photograph of hinge zone of the  $B_3$ -fold with well-developed axial foliation at the southernmost part of Menipa.

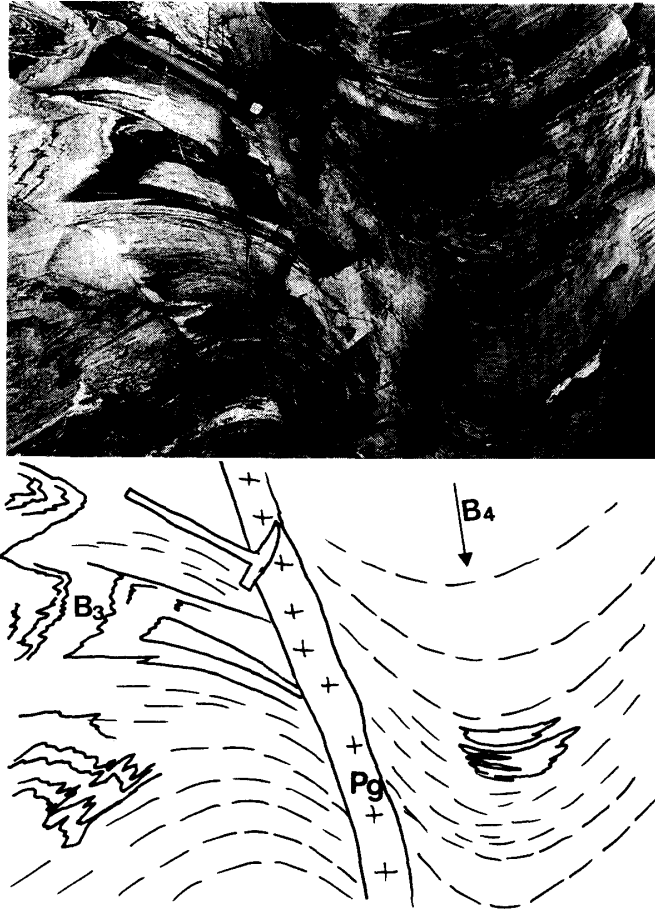


Fig. 13.  $B_3$ -isoclinal fold ( $B_3$ ) refolded by  $B_4$ -open fold ( $B_4$ ) at the northeastern corner of Walnumfjellet (locality no. 91010301). Pegmatitic granite dyke (Pg, pegmatite II after OWADA et al., 1991, 1992) is intruded into along the axial foliation of the  $B_4$ -fold.

appear to have resulted from the NNE-SSW compression during the  $D_4$  stage.

### 3.5. E-W compression resulting in N-S trending fold ( $D_5$ stage)

The deformation of the  $D_5$  stage is characterized by the formation of a N-S trending fold ( $B_5$ ) of pre- $S_5$ -foliations (Fig. 2) and by refolding of pre- $D_5$ -folds such as  $B_4$ - and  $B_3$ -folds (Figs. 16 and 17). The  $B_5$ -folds form open to gentle shapes with subvertical axial foliation ( $S_5$ ). Some of the  $D_5$ -folds are geological map scale antiform and synform. The  $D_5$ -folding may have been attributed to E-W compression.

### 3.6. NE-SW trending folding resulting from NW-SE compression ( $D_6$ stage)

The deformation of the  $D_6$  stage is characterized by the formation of NE-SW trending folds ( $B_6$ ) of the pre- $D_6$ -structures such as  $B_5$ - and  $B_4$ -folds (southern part of Austkampane in Fig. 1). The  $B_6$ -folds form gentle shapes with subvertical axial foliation ( $S_6$ ). Some of the  $D_6$ -folds are geological map scale antiforms and synforms (Figs. 1 and 2). The  $D_6$ -folding may have been due to NW-SE compression.

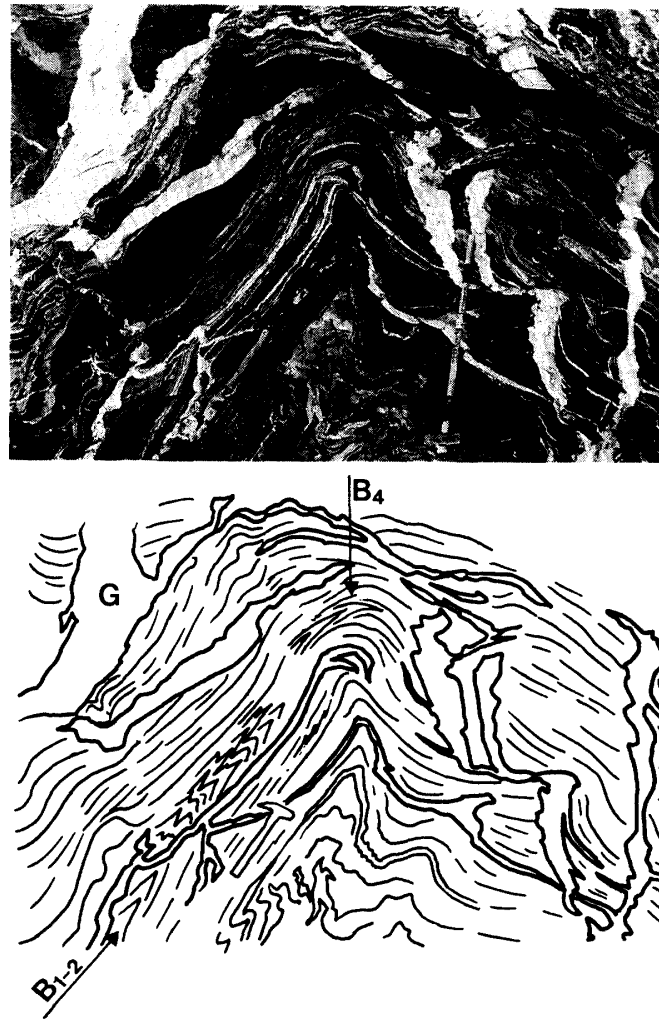


Fig. 14.  $B_4$ -fold ( $B_4$ ) with  $D_4$ -granite vein and dyke (G, pegmatite II after OWADA *et al.*, 1991, 1992) in the northern part of Lunckeryggen (locality no. 91011405), showing open shape and refolding  $B_{1-2}$ -fold ( $B_{1-2}$ ).

### 3.7. Non-foliated granite intrusion ( $D_7$ stage)

The deformation of the  $D_7$  stage is characterized by non-foliated granite and syenite intrusives (OWADA *et al.*, 1991; SAKIYAMA *et al.*, 1988) cutting across the pre-existing structures (Fig. 18). The granite and syenite occur as stocks, dykes and veins (OWADA *et al.*, 1991; SAKIYAMA *et al.*, 1988) and are the product of the last stage of the tectono-metamorphic history of the SRM. ASAMI *et al.* (1992) suggest that the metamorphic conditions of the  $D_7$  stage were around 550°C and 300 MPa, using stability of an And + Sil + Ms + Qtz association in pelitic gneisses adjacent to the  $D_7$ -granitic intrusives (ASAMI *et al.*, 1992). The mineral associations result from contact metamorphism with the  $D_7$ -intrusives.

Large Ky + Qtz porphyroblasts with random orientation are rarely found, growing across  $S_3$ -mylonitic foliation in the matrix of  $D_3$ -leucocratic granitic mylonites from the NE terrane (Fig. 11C). The leucocratic granites intruded into pelitic gneiss consisting of Grt +

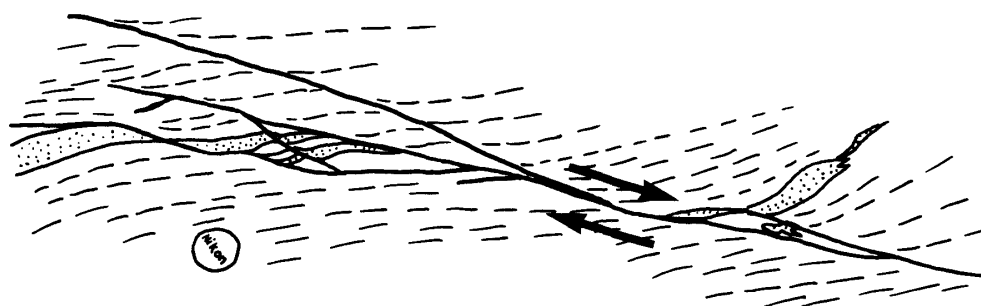
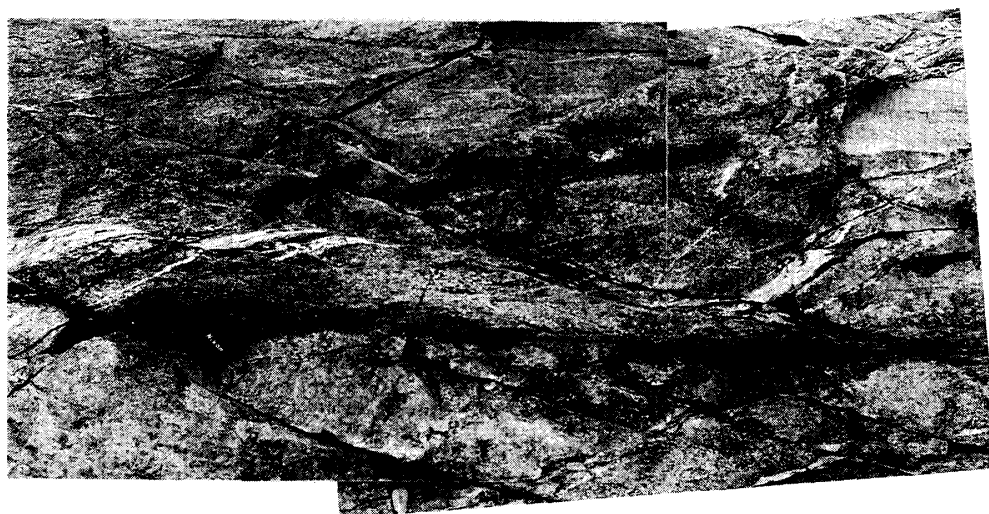


Fig. 15.  $D_4$ -minor shear zone cutting  $S_2$ -foliation of mylonitic tonalite from the southern part of Walnumfjellet (locality no. 91010103). The shear zone with refracted pre- $S_4$ -foliation has a monoclinic symmetry and are with top-to-the-N shear sense along steeply southward-inclined planes. The lens cap of the camera is 5.2 cm in diameter.

$Bt \pm Sil + Pl + Kfs + Qtz$ , and then were mylonitized during the  $D_3$  stage. However, preferred orientation is not clear in the leucocratic mylonites, except for shape preferred orientation of strongly elongated quartz ribbons defining the  $S_3$ -foliation. The porphyroblasts show oval, prismatic or spindle shapes in the leucocratic matrix dominated by  $Pl + Kfs + Qtz$  with small amounts of  $Ms + Grt$ . Each porphyroblast grain consists of a kyanite grain mantled by quartz (Fig. 11C). The long axis of the kyanite is parallel to that of the porphyroblast. The  $Ky + Qtz$  porphyroblasts do not have preferred dimensional and lattice orientations, suggesting that ductile deformation did not occur after the porphyroblast formation. Such a mode of occurrence and the fabrics of the porphyroblasts indicate that they were produced under non-deformational conditions in the kyanite-stable field after the  $D_3$ -mylonitization.

ASAMI and SHIRAISHI (1987) and ASAMI *et al.* (1992) stated that a retrograde kyanite-forming reaction involved the breakdown of garnet in pelitic gneisses under static conditions during a regional retrograde metamorphic stage. The retrograde kyanite is restricted to biotite aggregate which penetrates into garnet grains and with which garnet grains are fringed (ASAMI and SHIRAISHI, 1987). However, the kyanite in the porphyroblast is never in

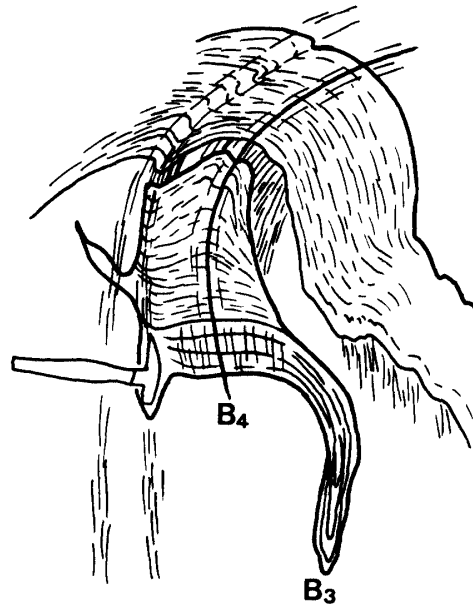


Fig. 16. Curve in  $B_4$ -fold axis ( $B_4$ ) resulting from  $D_5$ -folding at the southern end of Menipa (locality no. 91012504). The  $B_4$ -fold refolded  $B_3$ -fold ( $B_3$ ) of layered gneiss.

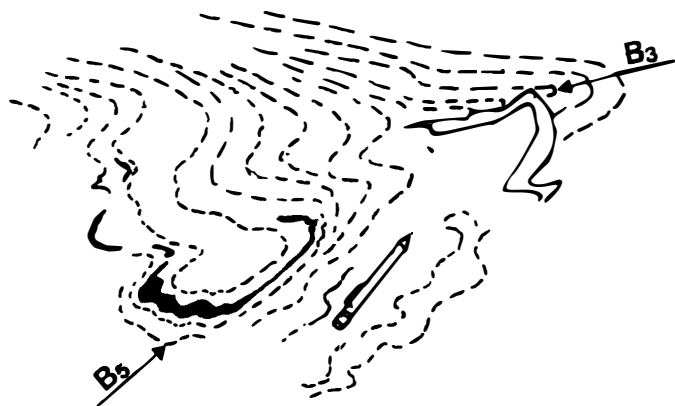
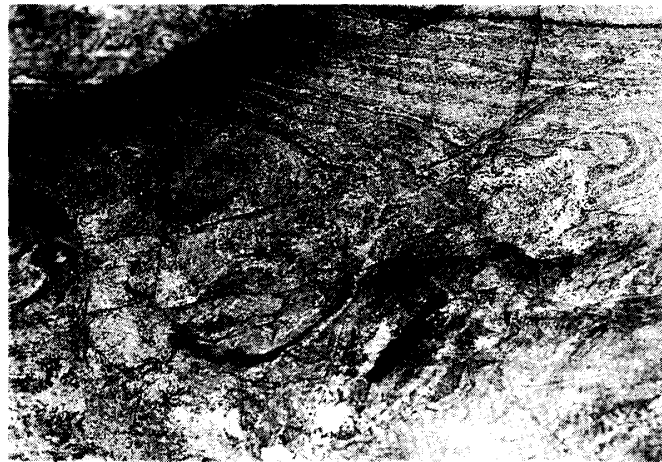


Fig. 17.  $B_5$ -fold ( $B_5$ ) refolding  $B_3$ -fold ( $B_3$ ) of layered gneiss from the southern end of Austkampane (locality no. 91020201).

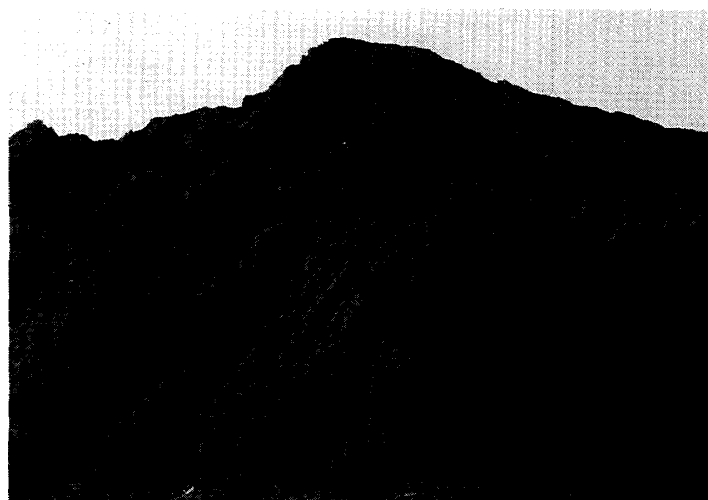


Fig. 18.  $D_7$ -granite dykes (light colored, steeply inclined to the left) cutting layered gneiss with pre- $D_7$ -structure (subhorizontal in this outcrop) at the southern end of Austkampane (locality no. 91012802).

direct contact with biotite and garnet, which are sporadically scattered in the mylonites but not near the porphyroblasts. Most of the garnets are embayed and replaced by biotites, showing that breakdown of garnet occurred. Many garnets fracture, and the fractures in the garnets are filled with biotites. The biotites formed through the breakdown of garnet define the  $S_3$ -mylonitic foliation, except for those in the embayments and fractures of the garnets. From the occurrences of the garnet, biotite and porphyroblast, the random-oriented and undeformed kyanites appear to be related to another metamorphic stage during the last stage ( $D_7$ ) after the retrograde kyanite formation ( $D_3$ ).

Many mylonites formed during  $D_2$  to  $D_3$  stages have granoblastic texture of recrystallized fine-grained minerals, quartz ribbons with strongly elongated shape but consisting of subequant to equigranular quartz grains (Figs. 7B, 11B and 11C). The quartz ribbons show slight undulatory extinction, suggesting almost strain-free conditions. Biotite defining the mylonitic foliations and asymmetrical structures is replaced by random-oriented and undeformed biotite, which cuts the mylonitic foliations (Figs. 7D and 11B). Therefore, preferred orientation is not clear in the mylonites, except for shape preferred orientation of strongly elongated quartz ribbons which define the  $S_2$ - or  $S_3$ -mylonitic foliations. Also, asymmetrical structures such as S, C and C' surfaces are present but only faintly visible in the mylonites (Figs. 7D and 11B). These appear to have been due to reheating or annealing after the mylonitization. The strain-free quartz ribbons and random-oriented kyanites and biotites cutting the  $S_3$ -foliation were undeformed after their formation. Therefore, their formation and the reheating may have resulted from the contact metamorphism with the non-foliated  $D_7$ -granite as shown by ASAMI *et al.* (1992).

The  $D_7$  stage granite yields a Rb-Sr whole rock isochron age of *ca.* 500 Ma, which has been regarded as the age of the intrusion (TAKAHASHI *et al.*, 1990).

#### 4. Summary

The structural evolution of the central part of the SRM is divided into seven stages,

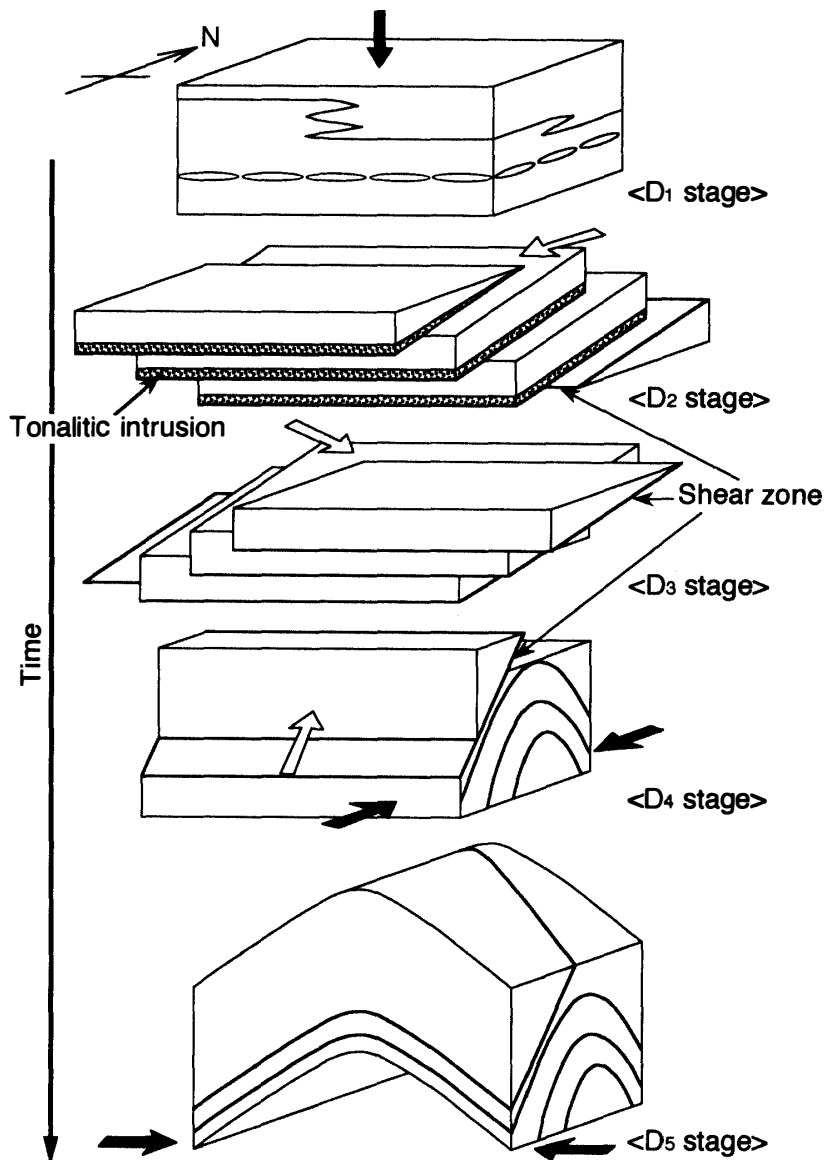


Fig. 19. Schematic diagram illustrating the structural evolution metamorphic and intrusive rocks from the central Sør Rondane Mountains which occurred during the D<sub>1</sub> to D<sub>5</sub> stages. Solid arrows show compressional stresses. Open arrows indicate shear directions (displacement vectors) lying within the shear planes.

from D<sub>1</sub> to D<sub>7</sub>, based on their characteristics of deformation, metamorphism and igneous activity (Table 1 and Fig. 19). It has been clarified that the metamorphic history of the central part of the SRM is divided into three stages, prograde metamorphic peak stage, retrograde metamorphic stage related to its exhumation and contact metamorphic stage. The metamorphism of the former two stages has not occurred only with ductile deformation but also with various kinds of magmatic intrusion. The D<sub>1</sub> stage before the tonalite intrusion stage is considered to correspond to the prograde metamorphic peak stage. The retrograde metamorphism and exhumation of the lower crustal rocks began at the D<sub>2</sub> stage

associated with the intrusion of the tonalite which was subsequently intensely mylonitized. The  $S_2$ -mylonitic foliation produced immediately after the tonalite intrusion was formed parallel to the planes along which the tonalite magma was emplaced. These imply that the initial stage of the exhumation tectonics of the SRM rocks resulted from the rise and intrusion of the tonalite magma, and that the  $D_2$ -shearing during the exhumation controlled and enhanced the tonalite intrusion along the shear planes (Fig. 19). Because the mylonitization and tonalite intrusion were caused by the top-to the SW to S displacement along the planes dipping to the S, the exhumation may have occurred in an extensional tectonic regime (Fig. 19). Therefore, the  $D_2$ -deformation may have been related to the rifting accompanying large-volume intrusion of tonalite magma (SHIRAISHI *et al.*, 1991). Subsequently, the  $D_3$ -mylonitization was caused by the top-to the SE displacement of the SRM rocks in another extensional tectonic regime (Fig. 19).

After these mylonite-forming tectonics, poly-stage folding occurred in some compressional tectonic regimes. The NNE-SSW compressional stress acted on the SRM rocks after the  $D_3$  stage and resulted in the WNW-ESE trending folds and minor thrusts with top-to the N sense (Fig. 19). The central SRM rocks was emplaced under greenschist facies conditions during this stage before the contact metamorphism with the  $D_7$ -granites. Subsequently the E-W compressional stress worked during the  $D_5$  stage (Fig. 19), and then NW-SE compression resulted in the  $D_6$ -folding. During the last stage ( $D_7$  stage) of the structural evolution of the central SRM, the non-foliated 500 Ma granite intrusion accompanied a thermal event (ASAMI *et al.*, 1992) and the metamorphic grade increased from greenschist facies to amphibolite facies.

### Acknowledgments

We are grateful to members of JARE-32 and -31 and the crew of the icebreaker SHIRASE for their support during the 1990–1991 season. Drs. Y. OSANAI, H. ISHIZUKA, Y. SAKIYAMA, Y. TAKAHASHI, Y. TAINOSHO, N. TSUCHIYA, M. ASAMI and M. ISHIKAWA are acknowledged for their invaluable discussions and helpful advice.

### References

- ASAMI, M and SHIRAISHI, K. (1987): Kyanite from the western part of the Sør Rondane Mountains, East Antarctica. *Proc. NIPR Symp. Antarct. Geosci.*, **1**, 150–168.
- ASAMI, M., OSANAI, Y., SHIRAISHI, K. and MAKIMOTO, H. (1992): Metamorphic evolution of the Sør Rondane Mountains, East Antarctica. *Recent Progress in Antarctic Earth Science*, ed. by Y. YOSHIDA *et al.* Tokyo, Terra Sci. Publ., 7–15.
- BERTHÉ, D., CHOUKROUNE, P. and JÉGOUZO, P. (1979): Orthogneiss, mylonite and non-coaxial deformation of granites: The example of the South Armorican Shear Zone. *J. Struct. Geol.*, **1**, 31–42.
- ISHIZUKA, H. and KOJIMA, H. (1987): A preliminary report on the geology of the central part of the Sør Rondane Mountains, East Antarctica. *Proc. NIPR Symp. Antarct. Geosci.*, **1**, 113–128.
- ISHIZUKA, H., ASAMI, M., GREW, E.S., KOJIMA, H., MAKIMOTO, H., MORIWAKI, K., OSANAI, Y., OWADA, M., SAKIYAMA, T., SHIRAISHI, K., TAINOSHO, Y., TAKAHASHI, Y., TOYOSHIMA, T. and TSUCHIYA, N. (1993): Geological map of Bergersenfjellet. *Antarct. Geol. Map Ser.*, Sheet 33 (with explanatory text 10 p.). Tokyo, Natl Inst. Polar Res.
- KOJIMA, S. and SHIRAISHI, K. (1986): Note on the geology of the western part of the Sør Rondane Mountains, East Antarctica. *Mem. Natl Inst. Polar Res.*, Spec. Issue, **43**, 116–132.

- KRETZ, R. (1983): Symbols for rock-forming minerals. *Am. Mineral.*, **68**, 277-279.
- LISTER, G.S. and SNOKE, A.W. (1984): S-C mylonites. *J. Struct. Geol.*, **6**, 617-638.
- OSANAI, Y., TAKAHASHI, Y. and SAKIYAMA, T. (1988): High-grade metamorphic rocks from the central part of the Sør Rondane Mountains, East Antarctica (abstract). *Proc. NIPR Symp. Antarct. Geosci.*, **2**, 170.
- OSANAI, Y., TAKAHASHI, Y., SHIRAIISHI, K., SAKIYAMA, T., TAINOSHO, Y., TSUCHIYA, N. and ISHIZUKA, H. (1991): Chemical features of metamorphic rocks from the central part of the Sør Rondane Mountains, East Antarctica. Abstracts: Sixth International Symposium in Antarctic Earth Sciences. Tokyo, Natl Inst. Polar Res., 468-473.
- OSANAI, Y., SHIRAIISHI, K., TAKAHASHI, Y., ISHIZUKA, H., TAINOSHO, Y., TSUCHIYA, N., SAKIYAMA, T. and KODAMA, S. (1992): Geochemical characteristics of metamorphic rocks from the central Sør Rondane Mountains, East Antarctica. *Recent Progress in Antarctic Earth Science*, ed. by Y. YOSHIDA *et al.* Tokyo, Terra Sci. Publ., 17-27.
- OWADA, M., TOYOSHIMA, T., SHIRAIISHI, K., OSANAI, Y., TAINOSHO, Y. and TAKAHASHI, Y. (1991): Late Proterozoic to early Paleozoic magmatism in the Sør Rondane Mountains, East Antarctica. Abstracts: Sixth International Symposium in Antarctic Earth Sciences. Tokyo, Natl Inst. Polar Res., 474-475.
- OWADA, M., TOYOSHIMA, T., SHIRAIISHI, K., OSANAI, Y., TAINOSHO, Y., TAKAHASHI, Y., SAKIYAMA, T. and MATSUMOTO, Y. (1992): Plutonic rocks from the central part of the Sør Rondane Mountains, East Antarctica. *Commemorative Papers for Professor Y. MATSUMOTO, Exploration of volcanoes and rocks in Japan, China and Antarctica*, Yamaguchi, 507-514.
- PONCE DE LEON, M.I. and CHOUKROUNE, P. (1980): Shear zones in the Iberian Arc. *J. Struct. Geol.*, **2**, 63-68.
- SAKIYAMA, T., TAKAHASHI, Y. and OSANAI, Y. (1988): Geological and petrological characters of the plutonic rocks in the Lunckeryggen-Brattnipene region, Sør Rondane Mountains, East Antarctica. *Proc. NIPR Symp. Antarct. Geosci.*, **2**, 80-95.
- SHIRAIISHI, K. and KAGAMI, H. (1989): Preliminary geochronological study of granulites from the Sør Rondane Mountains—A comparison of Rb-Sr and Sm-Nd ages—. *Proc. NIPR Symp. Antarct. Geosci.*, **3**, 152.
- SHIRAIISHI, K. and KOJIMA, S. (1987): Basic and intermediate gneisses from the western part of the Sør Rondane Mountains, East Antarctica. *Proc. NIPR Symp. Antarct. Geosci.*, **1**, 129-149.
- SHIRAIISHI, K., ASAMI, M., ISHIZUKA, H., KOJIMA, H., KOJIMA, S., OSANAI, Y., SAKIYAMA, T., TAKAHASHI, Y., YAMAZAKI, M. and YOSHIKURA, S. (1991): Geology and metamorphism of the Sør Rondane Mountains, East Antarctica. *Geological Evolution of Antarctica*, ed. by M.R.A. THOMPSON *et al.* Cambridge, Cambridge Univ. Press, 77-82.
- SHIRAIISHI, K., OSANAI, Y., TAINOSHO, Y., TAKAHASHI, Y., TSUCHIYA, N., KOJIMA, S., YANAI, K. and MORIWAKI, K. (1992): Geological map of Widerøefjellet. *Antarct. Geol. Map Ser.*, Sheet 32 (with explanatory text 20 p.). Tokyo, Natl Inst. Polar Res.
- TAKAHASHI, Y., ARAKAWA, Y., SAKIYAMA, T., OSANAI, Y. and MAKIMOTO, H. (1990): Rb-Sr and K-Ar whole rock ages of the plutonic bodies from the Sør Rondane Mountains, East Antarctica. *Proc. NIPR Symp. Antarct. Geosci.*, **4**, 1-8.
- TOYOSHIMA, T., OWADA, M. and SHIRAIISHI, K. (1991): Structural evolution of metamorphic and intrusive rocks of the Sør Rondane Mountains, East Antarctica. Abstracts: Sixth International Symposium in Antarctic Earth Sciences. Tokyo, Natl Inst. Polar Res., 604-605.
- VAN AUTENBOER, T. (1969): Geology of the Sør Rondane Mountains. *Geologic Maps of Antarctica*, ed. by C. CRADDOCK *et al.* New York, Am. Geogr. Soc., Sheet 8, Pl. VIII (Antarctic Map Folio Ser., Folio 12).
- VAN AUTENBOER, T. and LOY, W. (1972): Recent geological investigations in the Sør Rondane Mountains, Belgicafjella and Sverdrupfjella, Dronning Maud Land. *Antarctic Geology and Geophysics*, ed. by R.J. ADIE. Oslo, Universitetsforlaget, 563-571.

(Received May 8, 1995; Revised manuscript received June 6, 1995)